Published by Avanti Publishers

Global Journal of Energy Technology Research Updates

ISSN (online): 2409-5818

Energy, Exergy and Exergo-Economic Analysis of an OTEC Power Plant Utilizing Kalina Cycle

Giuseppe Basta, Nicoletta Meloni, Francesco Poli*, Lorenzo Talluri and Giampaolo Manfrida

University of Florence, Firenze, Italy

ARTICLE INFO

Article Type: Research Article

Keywords:
OTEC
Kalina
Exergy
Water-ammonia
Exergo-economic

Timeline:
Received: August 25, 2021
Accepted: October 15, 2021
Published December 28, 2021

Citation: Basta G, Meloni N, Poli F, Talluri L, Manfrida G. Energy, Exergy and Exergo-Economic Analysis of an OTEC Power Plant Utilizing Kalina Cycle. Glob J Energ Technol Res Updat. 2021; 8: 1-18.

DOI: https://doi.org/10.15377/2409-5818.2021.08.1

ABSTRACT

This study aims to analyse an Ocean Thermal Energy Conversion (OTEC) system through the use of a Kalina Cycle (KC), having a water-ammonia mixture as a working fluid. KC represents a technology capable of exploiting the thermal gap of ocean water. This system was then compared with OTEC systems, which exploit ammonia, R134A and butane-pentane mixture as working fluid. The comparison was carried on through energy analysis, exergetic analysis, and exergo-economic analysis using the EES (Engineering Equation Solver) software. For each case study, cost rates and auxiliary equations were evaluated for all components and the mass flow rate and unit exergy cost for each stream. The results showed that the KC with water-ammonia as working fluid achieves the best exergo-economic performance among the examined cycles. The cost of electricity produced through KC using water - ammonia mixture was found to be 26,66 c€/kWh. The thermal efficiency and the exergetic efficiency were calculated and the withdrawal depth of ocean water was considered. The efficiencies resulted to be 3.68% for the thermal efficiency and 95.96% for the exergetic efficiency.

*Corresponding Author
Email: francesco.poli1@stud.unifi.it
Tel: +39 3475996289

1. Introduction

The simultaneous decrease of fossil resource availability and the increase in the level of pollutant emissions have raised global efforts towards the rise of the contribution of renewable energy sources in the overall energy transformation.

Seawater covers about 69% of the earth's surface so, in this context, the energy available in the sea has enormous potential and allows different forms of exploitation.

The main physical phenomena associated with the transport of energy from the sea are waves, currents, tides, and thermal gradients.

Among these sources, the Ocean Thermal Energy Conversion (OTEC) technology exploits the temperature difference between the warm surface and the deep cold seawater to produce electricity through thermodynamic conversion using a suitable power cycle.

Between 1971 and 2018, it was estimated that global energy consumption increased by 2.6 times reaching an energy production of $1.67 \cdot 10^{14}$ kWh in 2018 [1].

The global availability of ocean thermal energy is estimated to be about $4.4 \cdot 10^{16}$ kWh per year [2].

In particular, this huge potential is mainly located in the ocean waters located around the tropics and in the correspondence of the Gulf Stream.

In these locations, the temperature difference between the warm and the cold seawater is typically in the range between 22°C and 26°C, due to the surface water temperature of about 28-30°C and the deep-water temperature of approximately 4-6°C [3].

Modern OTEC systems can rely on an open or a closed cycle.

The main advantage of the closed cycle is the possibility to select the working fluid to limit the size of the system components.

Conversely, the main disadvantage is the requirement of large heat exchangers made of expensive materials such as titanium to reliably operate in a chemically aggressive environment such as the sea.

For these reasons, it is necessary to improve the efficiency of the system.

Many kinds of operating fluids have been tested.

The working fluid must present a low-boiling temperature like organic fluids and refrigerants as R22 (Republic of Nauru plant), ammonia (Tokunoshima plant) and R32 (Kiribati Island plant) [4].

The efforts of the researchers have focused on islands and archipelagos, especially those far from the mainland since they appear as a very effective place to develop and test new and renewable energy technologies.

OTEC plants can be useful for islands that are frequently disconnected from a national power grid supply and therefore they require an alternative and reliable power supply source.

Moreover, unlike most other renewable technologies, it presents stable and continuous working conditions due to the temperature stability of ocean water layers [5].

The first OTEC plant was installed in Hawaii in 1979 with a rated capacity of 50kW [6].

Currently, there are only micro-OTEC operating plants all over the world and the biggest is located in Makai, Hawaii.

It has an installed power of 100kW and can supply energy for 120 houses [7].

In Kiribati Island, the Korean Research Institute of Ships and Ocean Engineer (KRISO) has developed an OTEC plant with a rated capacity of 1 MW.

It is supposed to be a demonstrative plant for one year and, depending on the success of the project, it will become operational [8].

2. Component and Cycle Configuration

The KC cycle was schematized with nine main components, each of which was simulated through thermodynamic, exergy, and exergo-economic analysis as per literature.

In addition, concerning the condenser and evaporator, the sizing of the components used for heat exchange between the working fluid and seawater was performed to optimize the conversion process.

The main components of the KC cycle (Fig. **1**), realized for this study, are:

1. Condenser
2. Low-Temperature Regenerator (LTR)
3. High-Temperature Regenerator (HTR)
4. Evaporator
5. Vertical separator
6. Steam turbine
7. Mixer
8. Throttling valve
9. Recirculation Pump

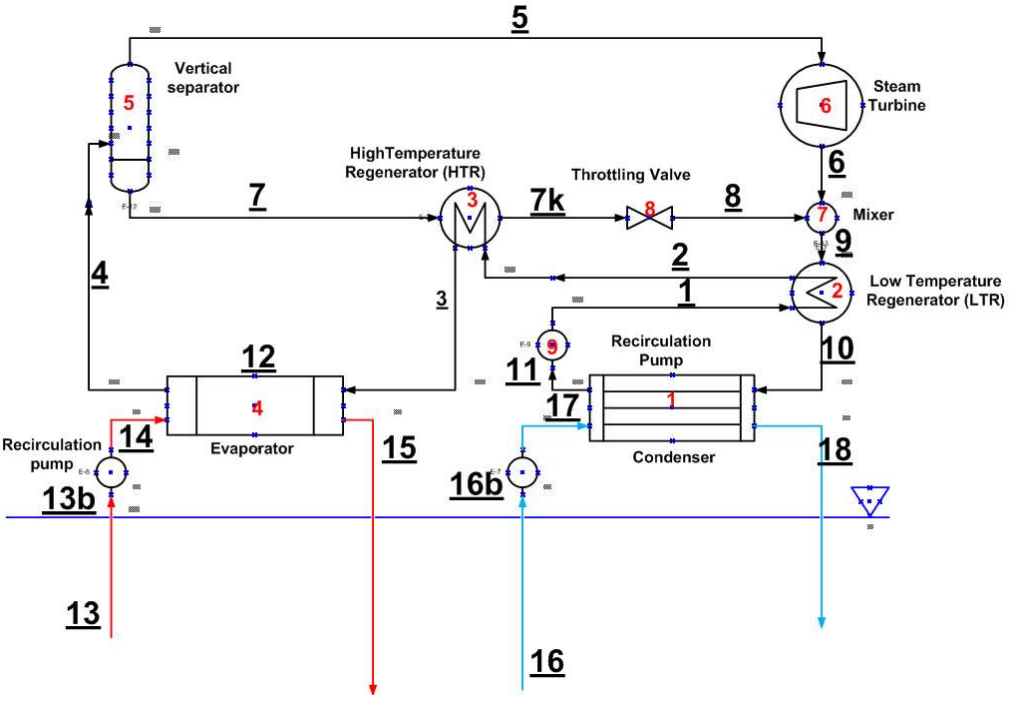

Figure 1: Design of the OTEC with using Kalina cycle.

Moreover, the ammonia fraction constitutes 85% of the overall compound.

Following, the working fluid cycle is examined and is depicted in Fig. (**1**). On the working fluid side, the NH3-H2O mixture enters the evaporator (component 4) under saturated fluid conditions at point 3 and exits under sub-saturated vapor conditions (point 4).

Therefore, the fluid not completely vaporized is sent to a vertical separator (component 5) that splits the compound into a vapor rich in ammonia (point 5) and a saturated liquid poor in ammonia.

The ammonia-rich vapor then leaves the separator (point 5) from the top and reaches the turbine that expands the vapor until the condenser pressure is achieved (point 6).

Following the expansion, the vapor is blended with the ammonia-poor liquid, reaching back to the initial compound ratios of the mixture.

Upstream of the condenser, the process encounters two regenerative heat exchangers.

The low-temperature regenerator (LTR) pre-cools the flow entering the condenser and allows to decrease the heat supplied to the evaporator.

An additional heat recovery process at high temperature (HTR) takes place among the flow exiting from the LTR and the fluid poor in ammonia.

As a consequence, a reduction of the external thermal energy is obtained, both for the condenser (points 10 - 11) and the evaporator (points 3 - 4).

A throttling valve (points 7k - 8) supplies the required pressure before the mixer.

The pump (points 11 - 1) provides the necessary pressure increase from the condenser pressure to the evaporator pressure [9].

As for the seawater circulation system, it simply consists of pumps that draw water at different depths depending on the required temperature and the component in which the heat exchange is carried out (condenser or evaporator).

The portion of water that exchanges heat with the NH3 - H2O mixture in the evaporator is drawn at a depth of 10 m above sea level with an estimated temperature of about 30 °C; while the water that cools the mixture in the condenser is drawn at a depth of 1000 m with a temperature of about 4.5 °C.

Under these conditions, the limit of energy efficiency is provided by Carnot's efficiency, which is shown in Eq. (1):

$$\eta_c = 1 - \frac{T_c^K}{T_h^K} \simeq 0.084 \quad (1)$$

Therefore, it is possible to state that the maximum ideal energy yield we can expect is about 8.4%.

Figure **2** shows the ocean water temperature profile as a function of depth, from which it can be seen that it does not exhibit a linear trend.

3. Energy Analysis

The energy analysis was performed by first analyzing the Kalina plant, assumed to be a closed system, and then the ocean water extraction plant, which, exchanging matter with the sea, was treated as an open system.

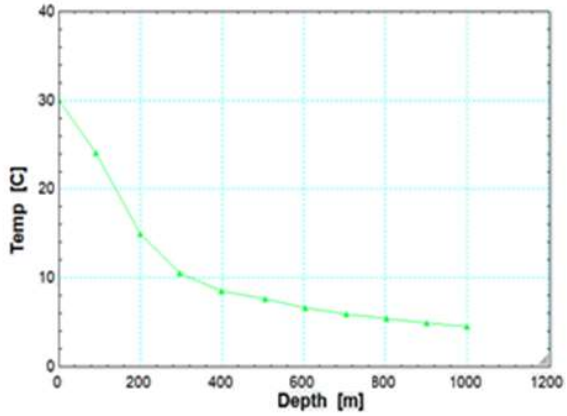

Figure 2: Ocean water temperature profile versus depth [6].

The components were treated with traditional mass and energy balances under steady-state conditions: closed loop for the KC and open-loop for the water circulation system.

Table 1: Thermodynamic values of stream.

Stream	P[bar]	T[K]	s[kJ/kgK]	h[kJ/kg]	m[kg/s]
1	7.400	279.1	0.0500	-80.07	42.11
2	7.400	283.3	0.1195	-60.54	42.11
3	7.400	285.9	0.1620	-48.43	42.11
4	7.400	300.7	2.3370	597.20	42.11
5	7.400	300.7	4.5560	1316.00	20.12
6	4.600	276.3	4.5780	1261.00	20.12
7	7.400	300.7	0.3075	-60.53	21.99
7k	7.400	295.7	0.2297	-83.72	21.99
8	4.600	286.8	0.2326	-83.72	21.99
9	4.600	286.3	2.3100	558.80	42.11
10	4.600	285.7	2.2420	539.30	42.11
11	4.600	279.0	0.0498	-80.52	42.11
12	7.400	293.1	0.2839	-13.13	42.11
13	1.994	302.7	0.4306	124.10	2168.00
13b	1.012	302.7	0.4306	124.00	2168.00
14	1.052	302.7	0.4306	124.00	2168.00
15	1.017	299.7	0.3890	111.40	2168.00
16	99.080	277.7	0.0687	28.74	2818.00
16b	0.999	277.7	0.0685	19.02	2818.00
17	1.245	277.7	0.0687	19.05	2818.00
18	1.133	279.9	0.1020	28.31	2818.00

3.1. Energy Analysis Kalina Cycle

The input data used for plant sizing are as follow:

Table 2: Entry data used for analysis purposes.

$W_{net} = 1000\ kW$	Net power output
$P_{evap} = 7.4\ bar$	Upper circuit pressure
$P_{cond} = 4.6\ bar$	Lower circuit pressure
$\dot{m}_{warm} = 2168\ \frac{kg}{s}$	Warm water mass flow rate
$\alpha = 0.85$	Ammonia mass fraction within the base
$\gamma = \frac{\dot{m}_{cold}}{\dot{m}_{warm}} = 1.3$	Cold water flow and Warm water flow ratio
$T_{13} = 302.75\ K$	Warm water temperature at suction point
$T_{16} = 277.65\ K$	Cold water temperature at suction point
$Range_e = 3\ K$	Warm water temperature difference at the inlet and outlet of the evaporator
$\Delta T_{app} = 2\ K$	Evaporator approach temperature
$\Delta T_{app\ LTR} = 3\ K$	Low-Temperature Regenerator approach temperature
$\Delta T_{app\ HTR} = 5\ K$	High-Temperature Regenerator approach temperature
$H_{cold} = 1000\ m$	Cold water suction point depth
$H_{warm} = 10\ m$	Warm water suction point depth
$\eta_t = 0.9$	Turbine isoentropic efficiency
$\eta_p = 0.9$	Isentropic pump efficiency

3.2. Evaporator and Condenser Sizing

The sizing of the evaporator and condenser was performed through an in-house developed procedure, which was derived from [10].

Since the original procedure provided as input only the fluids already present in EES, it was necessary to modify the procedure to treat as input fluids the water and the water-ammonia mixture (which, in addition to not being present in EES, is not treated exhaustively on REFPROP). This modification also allowed the development of additional procedures for calculating the viscosity, conductivity, vapor fraction, and specific heat of the water-ammonia mixture as a function of pressure, temperature, and the fraction of ammonia in the mixture (Fig. **3**) via the transport equations [11-14].

3.3. Exergetic Analysis

Exergetic analysis makes it possible to evaluate not only the efficiency of the energy systems evaluated but also to identify the sources of irreversibility (exergetic destructions) of each component, which hinder the performance of the system.

The standard definition of exergy is "the maximum work achievable by a system or process through interaction with its surroundings".

Eq. (2) supplies the general flow exergy equation at steady conditions, that can be calculated at any point of the system:

$$\dot{Ex}_t = \dot{m} \cdot [(h - h_0) - T_0\ (s - s_0)] \quad (2)$$

This definition points to exergetic analysis as the right tool to evaluate the maximum possible exploitation obtainable from a renewable resource of thermal nature, such as OTEC application [6].

a.1) **a.2)**

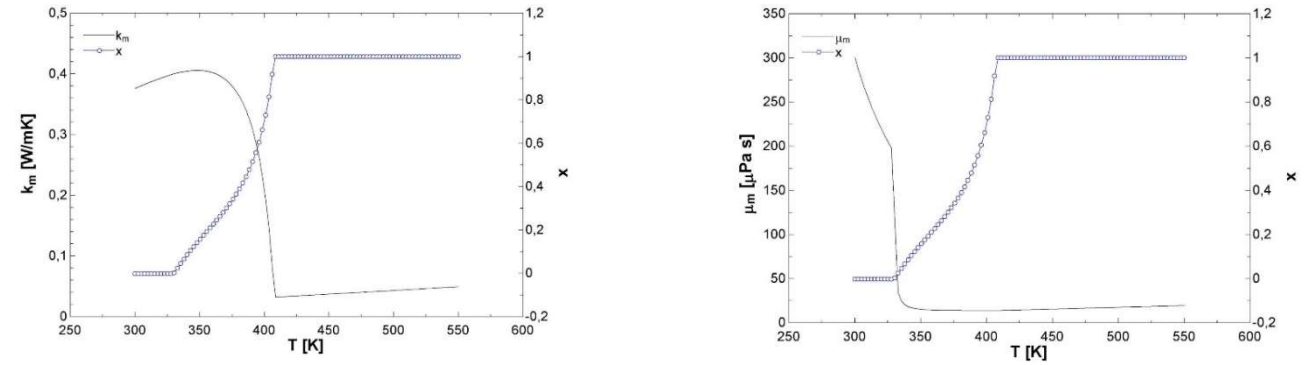

b.1) **b.2)**

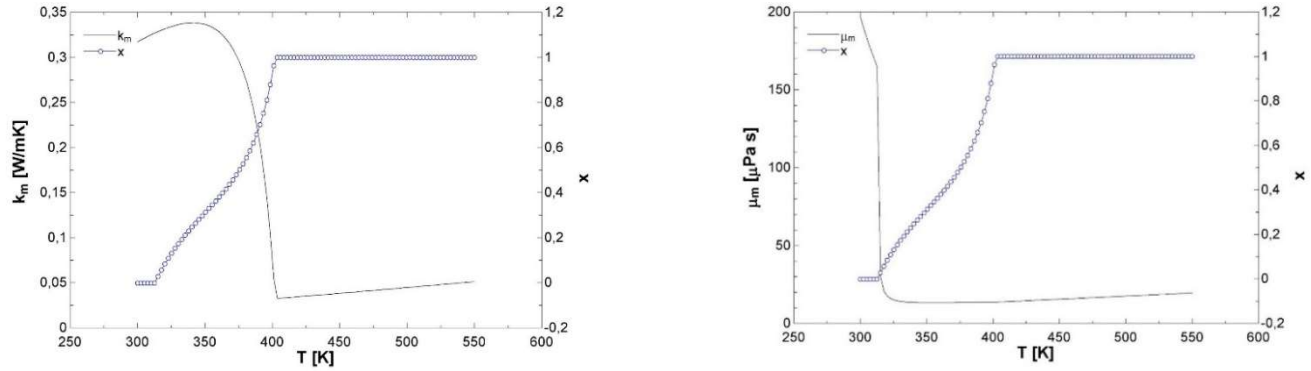

Figure 3: (**a.1**) Conductivity and vapour fraction as a function of temperature for a mixture with 40% ammonia - (**a.2**) Viscosity and vapour fraction as a function of temperature for a mixture with 40% ammonia – (**b.1**) Conductivity and vapour fraction as a function of temperature for a mixture with 50% ammonia - (**b.2**) Viscosity and vapour fraction as a function of temperature for a mixture with 50% ammonia.

By defining the exergetic destruction and losses of a system, it is possible to set the exergetic balance of each part of the system. The exergetic efficiency of a component is defined as the ratio between the exergy of the products and the exergy of the fuels, as shown in Eq. (3):

$$\eta_{Ex} = \frac{\dot{Ex}_p}{\dot{Ex}_F} \tag{3}$$

The exergetic efficiency for the studied OTEC system was calculated considering the geodetic jumps of ocean water extraction and is expressed in Eq. (4):

$$\eta_{dir,II} = \frac{W_{net} + W_{geo}}{\dot{Ex}_{in}} \tag{4}$$

Where:

$$\dot{Ex}_{in} = \dot{Ex}_{cold,in} + \dot{Ex}_{warm,in} - \dot{Ex}_{cold,out} - \dot{Ex}_{warm,out} \tag{5}$$

$$W_{geo} = \dot{m}_{cold}(h_{16} - h_{16b}) + \dot{m}_{warm}(h_{13} - h_{13b}) \tag{6}$$

W_{geo} in Eq. (6) is the energy required by the water to overcome the geodetic jump between the inlet suction pipeline and the water surface, $\dot{Ex}_{cold,in}$ and $\dot{Ex}_{cold,out}$ in Eq. (5) are the inlet and outlet cold water flow exergy at

the condenser pipelines respectively, and $\dot{Ex}_{warm,in}$ and $\dot{Ex}_{warm,out}$ are the inlet and outlet warm water flow exergy at the evaporator pipelines.

Eq. (4) represents a direct ($_{dir}$) method to evaluate the efficiency while an alternative, indirect ($_{ind}$) method is given in Eq. (7), as follow:

$$\eta_{ind,II} = 1 - \sum_{i} \dot{Ex}_{DLr,i} \tag{7}$$

Where:

$$\dot{Ex}_{DLr,i} = \frac{\dot{Ex}_{DL,i}}{\dot{Ex}_{in}} \tag{8}$$

$\dot{Ex}_{DLr,i}$ in Eq. (8) is the *relative flow exergy destruction or loss* (DL) within the i-th component given by the ratio between the flow exergy destruction or loss within the i-th component and the total flow exergy of the "fuel" entering the overall system.

Exergo-economics is the branch of thermodynamics that applies to a single component or an entire system and aims to identify the costs due to a process of energy transformation taking into account the irreversibility of the process itself [15].

The exergo-economic analysis combines exergetic and economic analysis to explain the cost build-up throughout the power plant process and to ultimately obtain the *levelized cost of electricity* (LCOE).

Particularly, through the combination of the exergy and economic analysis, it is possible to assess the cost-effectiveness of each component, allocating to each exergy stream a specific cost [16].

This type of analysis is carried out especially in the case of having to choose the best solution at the lowest possible cost.

The exergo-economic analysis of a system turns out to be effective above all when it is possible to compare it with one or more systems that operate under the same external conditions.

The applied economic model considers the instantaneous cost of each component in €/s.

Standard rules are applied to evaluate the value of Ż [€/s] from the Purchased Equipment Cost (PEC) [17].

The PEC of each component was determined through the correlations reported in the Turton procedure, which takes into account the characteristic size of the component to calculate its cost [17].

These correlations were incorporated into the program design in the form of a procedure called cbm.

Costs were discounted to 2019 values using CEPCI indices [18]. Therefore, the purchase cost was not calculated through the use of scaling factors.

The currency exchange rate from $ to € applied is 1.11 $/€.

Auxiliary costs, which are therefore not the purchase costs of the components, were included in the analysis as a function of the total purchase cost of the components; the costs that have the greatest influence on the analysis are shown below [9]:

- The total installation cost of OTEC system: 6%
- The total cost of piping: 7%
- Cost of instrumentation, controls, and electronic devices: 5%

- Civil works: 7%
- Engineering consulting and supervision costs: 6%
- Construction costs:3%
- Contingency Costs: 8%

Total fixed capital investment was then calculated as the sum of direct and indirect fixed capital investment, on which the start-up, maintenance, and insurance costs were dependent.

The Capital Recovery Factor (CRF) was calculated in order to consider the present value of the investment distributed in equal annual payments.

The formulation and assumptions considered are as follows:

Table 3: Assumptions for economic analysis.

$CRF = \frac{[i \cdot (1+i)^y]}{(1+i)^y - 1}$	Capital Recovery Factor
i = 0,10	Interest rate
y = 20	Expected lifespan [years]
$\phi = 1 + r_n$	Maintenance factor
$r_n = 0.06$	Nominal escalation rate
$N_h = 7000$	Annual operating hours [h/year] [4]

4. Results

4.1. Performance Analysis

The first analysis to be carried out is to assess the contribution that pumping power has on the net power output of the power station, due to friction losses in the water pipes.

Figure **4** shows (as a function of the flow rate of the cold fluid resource) the net power of the power plant, the gross power produced by the turbine, and the pumping work required to overcome the pressure drop in the piping.

From Figure **4**, it can be seen that there is a maximum of the power that can be obtained from the system, which is given by the combination of the trends of the gross turbine power (linear behaviour) and the power required by the pumps in the system (quadratic behaviour) as a function of the water flow rate in the cold pipe.

The subsequent analysis is aimed to evaluate the optimal specific power range and the overall efficiency of the power plant.

The specific power is defined as the ratio of the net power output to the chilled water mass flow rate:

$$\dot{W}_{sp} = W_{net}/\dot{m}_{cold}$$

The overall system efficiency is defined as the ratio between the net power and the heat exchanged at the evaporator.

$$\eta_{ciclo\ dir} = W_{net}/Q_{evap\ tot}$$

An analysis was conducted in search of the optimal specific power and efficiency, depending on the two most relevant design parameters of the plant, namely the mass flow ratio and the range at the evaporator.

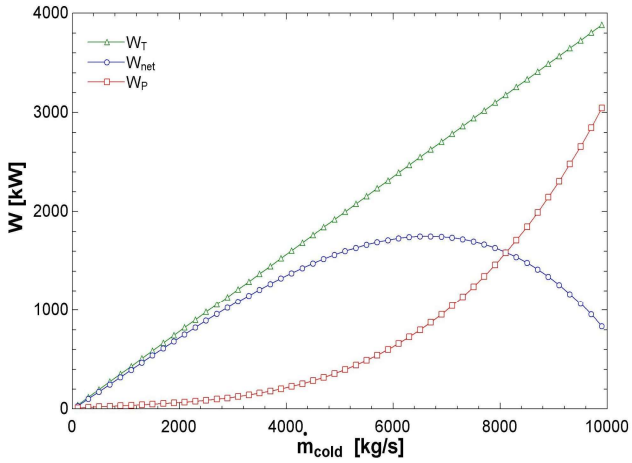

Figure 4: Net power as a function of cold-water flow rate (velocity inside the pipes of 1 m/s).

Figures **5** and **6** show the change in specific power and overall efficiency as a function of γ and range at the evaporator:

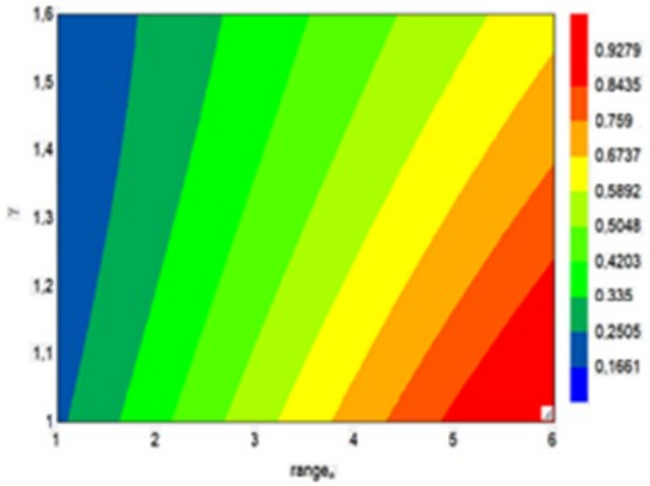

Figure 5: Specific power as a function of range$_e$ and γ.

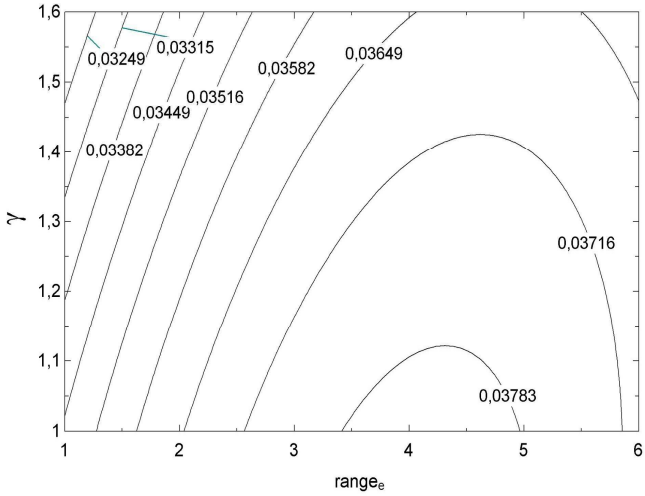

Figure 6: Overall efficiency as a function of range$_e$ and γ.

It is advantageous to use a higher hot water mass flow rate (compared to the cold-water flow rate) since pumping losses are mainly associated with the suction cold pipeline, which is much longer than a warm pipeline.

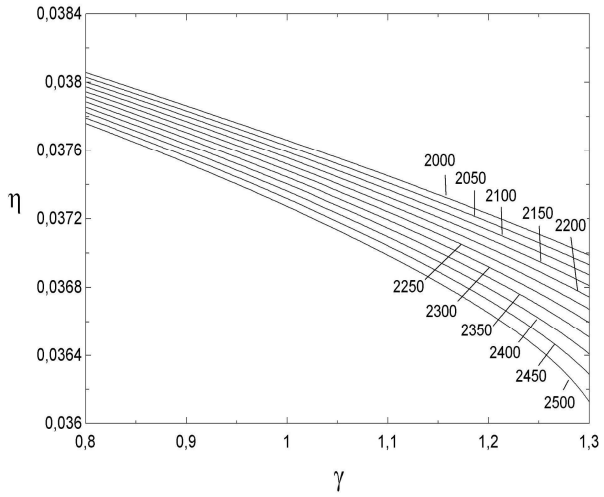

Figure 7: Efficiency trend as a function of a fixed range of hot water flow rate.

In Fig. (**7**) it is possible to observe the performance trend as a function of the variation of the range once the hot water flow rate is fixed.

This plot could be used for the regulation of the plant, and it is possible to notice that as the range increases for high hot water flow rates the efficiency of the system tends to decrease faster, while for lower flow rates there is a more linear trend.

4.2. Exergetic Analysis

The exergetic performance of the OTEC system resulted to be 95.96% considering a mass flow rate ratio $\gamma = 1.3$ and a temperature difference of the flow at the evaporator of 3°C.

As shown in Fig. (**8**), the most contribution to the efficiency and the irreversibility of the system is given by the condenser at which is attributed an exergetic destruction equal to 1.36% compared to the exergy at the inlet of the system.

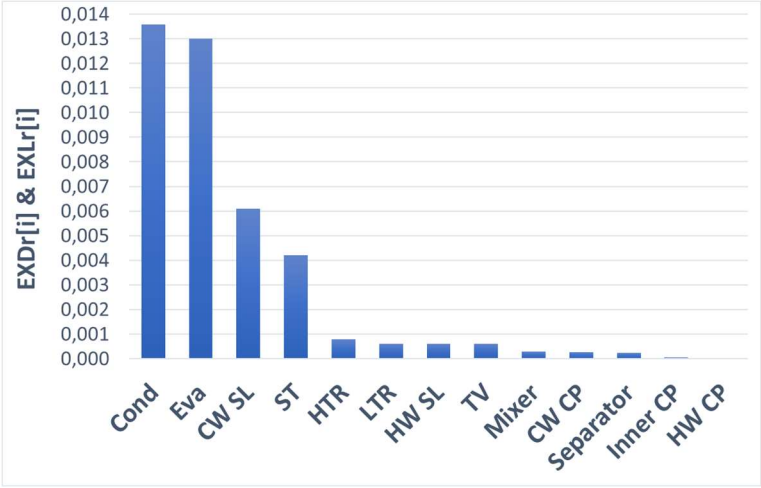

Figure 8: Exergy destruction and losses (γ= 1.3, range$_e$ = 3).

This is due to a non-optimal thermal match between the water-ammonia mixture and the cooling water.

Together with the condenser, the main exergy destruction sources have been attributed to the evaporator and the cooling water suction line.

These three components, bunched together, are responsible for exergy destruction and loss equal to 3.27%.

Given the fact that is not feasible a perform improvement about the exergetic losses that occur within the suction line, it is recommended to test alternative and more efficient solutions regarding the heat exchangers.

As it is shown in Fig. (**9**), the highest exergy efficiencies are reached for low values of $range_e$ at the evaporator.

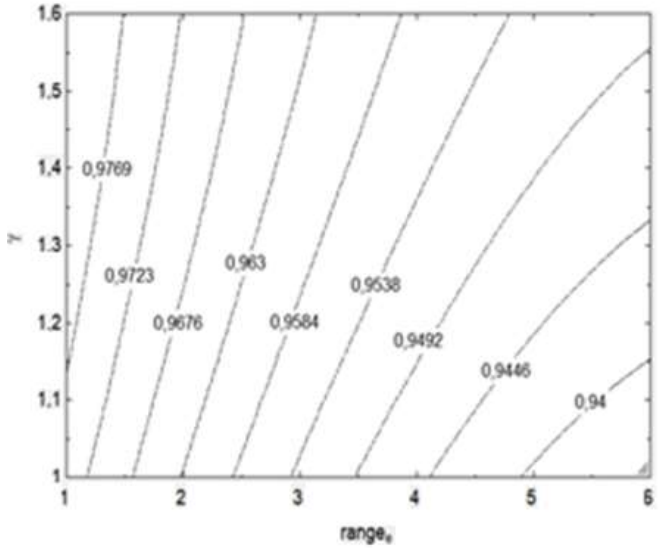

Figure 9: Exergy efficiency of the OTEC system as function of gamma and $range_e$.

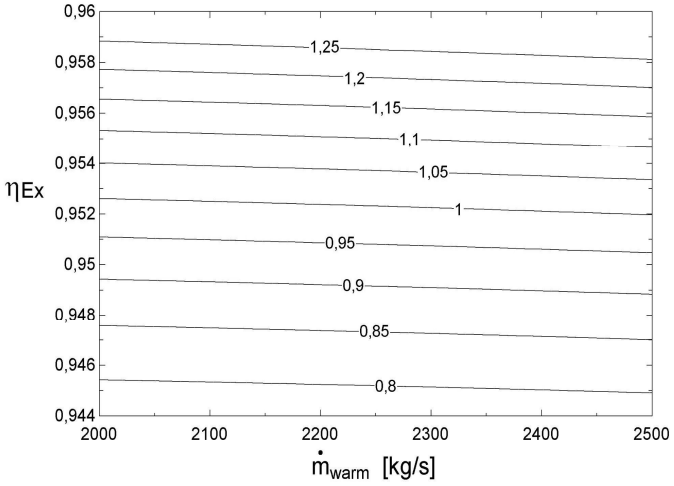

Figure 10: Exergy efficiency as a function of the cold water flow rate for each fixed gamma.

As shown in Fig. (**10**), the exergy efficiency has a linear slope and an almost constant behavior increasing the hot water mass flow rate when gamma is given.

It is noticeable that exergetic efficiency is not particularly influenced by the mass flow rate regulation, but rather the mass flow ratio.

4.3. Exergo-Economic Analysis

Lastly, following the thermodynamic and exergetic analysis, exergo-economic calculations have been carried out.

The obtained overall specific investment cost of the system has been estimated equal to 1980 € / kW.

Since the cost of the net power produced by the cycle relies on many inlet variables, a reference configuration has been considered as follow:

- $\gamma = 1.3$;
- $Range_e = 3$;
- The cost of flows at point 13 and 16 (suction points of hot water and cold water respectively) have been assumed equal to 0; and
- The electricity cost required by the pump is equal to the cost of electricity produced by the turbine.

Considering the aforementioned hypothesis, Table **4** shows the results obtained by the exergo-economic analysis of the OTEC system for the present case study.

Table 4: Exergo-economic analysis results.

Components	PEC [€]	$\dot{Z}$[€/s]
Condenser	$4.99 \cdot 10^6$	0.04275
Low Temperature Regenerator (LTR)	172012	0.001474
High Temperature Regenerator (HTR)	78000	0.0006683
Evaporator	$2.23 \cdot 10^6$	0.01908
Separator	42576	0.0003648
Steam turbine	$1.09 \cdot 10^6$	0.009324
Mixer	0	0
Throttling valve	0	0
KC Pump	12521	0.0001073
Hot water suction line pump	7020	0.00006014
Cold water suction line pump	19931	0.0001708
Cold water circuit	512808	0.004394
Hot water circuit	22291	0.000191

In terms of economic analysis, the condenser is the most expensive component followed by the evaporator (Table **4**).

It is possible to observe, from the top picture of Fig. (**11**), that the condenser is responsible for 67% of the purchase equipment cost of only the most onerous components, followed by the evaporator responsible for 30% and the high and low-temperature regenerators that contribute with 1% and 2% respectively.

The cost of the present components is mostly attributed to the large, required heat exchanger's surfaces that resulted to be 10457 m^2 for the condenser and 4954 m^2 for the evaporator.

a)

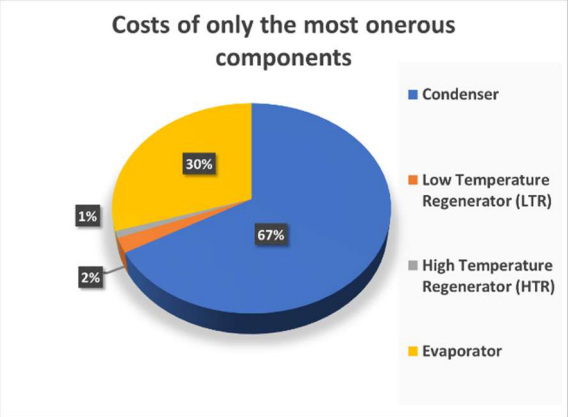

b)

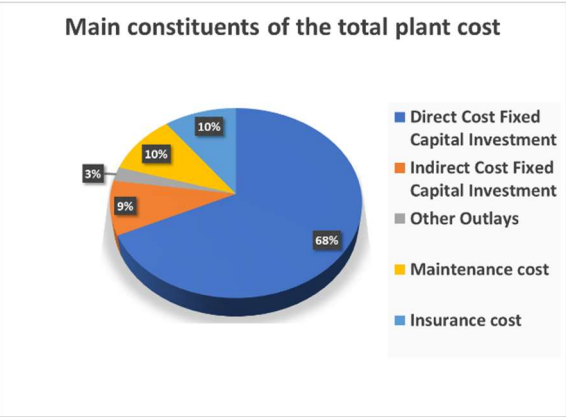

Figure 11: (**a**) Percentage weight of purchase cost of only the most onerous components of the system - (**b**) Percentage weight of the main items that constitute the required investment to realize the plant.

The initial total investment value resulted to be 1.98 M€ of which 68% is due to direct costs, that include:

- the total purchase cost of the main components;
- overall plant's piping cost;
- installing cost of the components;
- cost of electrical and control equipment; and
- cost of civil works.

The remaining main items are:

- maintenance costs (10%);
- insurance costs (10%);
- indirect costs, such as contingency and engineering consultancy costs (9%); and
- other costs (3%).

From an exergo-economic point of view, considering Ż (Table **4**), once again the same components are the biggest contributors, followed by the turbine.

The specific cost of the exergy product (*c_e*) associated with the power cycle turbine represents the cost of the OTEC power plant output, i.e. the cost of producing electricity.

In our case study, the production cost is 26.66 c€ / kWh (Fig. **12**), which is a rather high value compared to other systems, mainly due to the relatively low power and low conversion efficiency of the system.

Figure **12** shows economic comparisons with other OTEC systems that were modelled over the system described by *Bernardoni et al*. [2].

These systems were analyzed applying the same procedure, the same parameters for the economic analysis, and the same net power output system (1 MW), thus an economic comparison between them is strongly viable.

The ORC system exploiting R134a as working fluid is the most expensive system along with the system using NH_3 with a cost of 2.44 and 2.39 M€ respectively, while the butane-pentane system costs 2.19 M€ which is less expensive compared to the previews two.

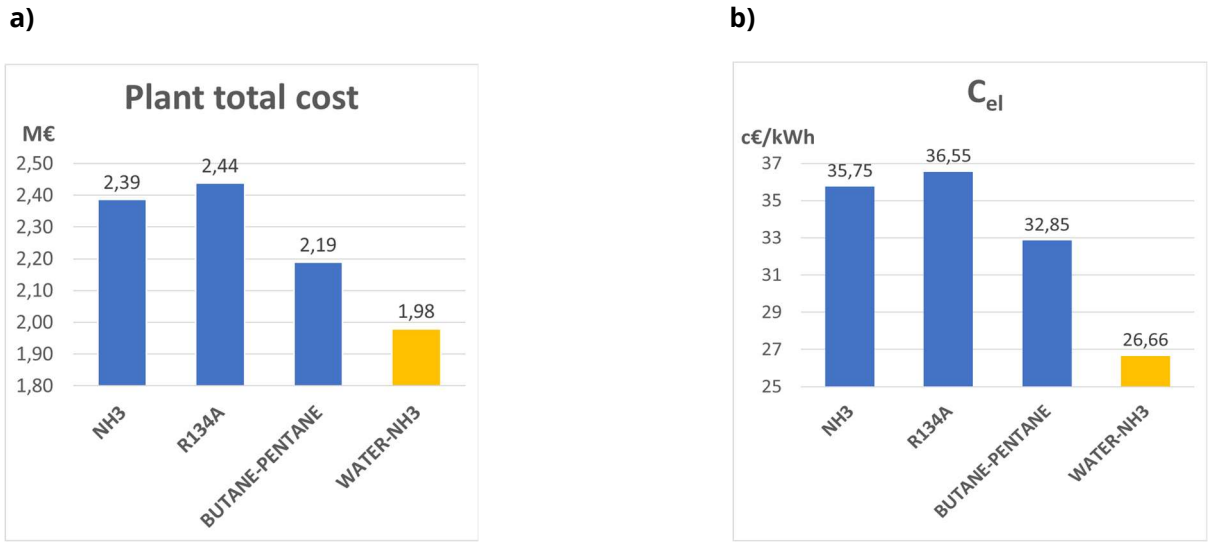

Figure 12:(**a**) Cost of OTEC system for each analysed system - (**b**) Cost of electricity produced for each analysed OTEC.

The studied system resulted to be the least expensive with a plant total cost equal to 1.98 M€.

Regarding the output electricity cost, the most expensive is R134a which has been evaluated 36.55 c€/kWh.

It's followed by NH_3 and butane-pentane with an expected cost of 35.75 c€/kWh and 32.85 c€/kWh respectively.

As we can expect, since each power plant has an output power of 1 MW the cost of electricity is proportional to the plant total cost. Thus, the least resulted to be the ammonia-water system with a cost equal to 26.66 c€/kWh.

5. Conclusions

This work has been modelled an OTEC system using KC with ammonia-water as working fluid through EES software.

The power plant has been designed to work with 1 MW as net power output.

The KC exploit an aqueous mixture with 85% of ammonia and a condenser that works with a 3°C range between the inlet and outlet temperature of warm water.

The temperature of inlet cold water has been considered 4 °C at 1000 m depth and the hot water inlet has been set at 29 °C at 10 m depth [3].

The isentropic efficiency of the steam turbine has been set at 0.9.

Energy, exergetic, and exergo-economic analyses were carried out, highlighting performance behaviours and sources of losses, as well as confirming the validity of the evaluated technology.

The thermo-fluid dynamics analysis allowed us to conclude that to obtain a relatively high efficiency of the system, the work of the cold-water pumps should be kept low.

In addition, it was possible to define appropriate values for the evaporator range and mass flow ratio to maximize the specific power output, which can be obtained maximising *Range_e* and minimazing γ.

The exergetic analysis made it possible to understand the origin of the main sources of loss and the irreversibility of the system.

Specifically, it was found that the main exergetic destructions occur in the condenser causing 1.36% of the total exergy input loss and 1.3% in the evaporator of the total exergy input, while the cold-water intake duct contributes with 0.61%.

Finally, the exergo-economic analysis allowed us to calculate the cost of electricity production in the system configuration.

The obtained value about electricity cost production of 26.66 c€/kWh is within the expected range, as confirmed in the literature [2] and the plant total cost resulted to be 1.98 M€.

The high value is mainly due to the low conversion efficiency of the plant (~3.68%), which is thermodynamically hampered by the low temperatures of the energy sources with which the Kalina cycle exchanges heat (evaporator T = 30 °C).

Other OTEC systems using different cycles and working fluids have been modelled following the same design in order to compare their exergo-economic results with the system under consideration.

Specifically, three other systems were considered using NH_3, R134a and butane-pentane mixture as working fluid.

The considered plant resulted to be the least expensive regarding the plant overall cost and the electricity production cost.

The analysis developed confirmed that OTEC plants could be a feasible solution for electricity production, as they can exploit a potentially inexhaustible 'free' green resource.

Nomenclature

c_e	Specific cost of the exergy product
CRF	Capital Recovery Factor
EES	Engineering Equation Solver
Ex	Exergy [kW]
H	Suction Depth [m]
HTR	High-Temperature Regenerator
I	Interest rate
k	Conductivity [W/m K]
KC	Kalina Cycle
LCOE	Levelized Cost Of Electricity
LTR	Low-Temperature Regenerator
$\dot{m}$	Mass flow rate [m/s]
N_h	Annual operating hours
ORC	Organic Rankine Cycle
OTEC	Ocean Thermal Energy Conversion
P	Pressure
PEC	Purchased Equipment Cost [€]
$Range$	Inlet and outlet temperature water difference at the heat exchangers [K]
r_n	Nominal escalation rate
W	Power [kW]

x	Vapor mass fraction
y	Years
$\dot{Z}$	Economic impact rate [€/s]

Greek

α	Ammonia mass fraction
γ	Mass flow ratio
η	Efficiency
μ	Viscosity [$\mu Pa\ s$]
ϕ	Maintenance factor

Subscripts/Superscripts

app	Approach
C	Carnot
cold	Cold water
cond	Condenser
Dir	Direct
DL	Destruction/Loss
$evap$	Evaporator
F	Fuels
geo	Geodetic
in	Inlet
Ind	Indirect
M	Mean
Net	Net
out	Outlet
P	Products
P	Pump
R	Relative
sp	Specific
t	Turbine
TOT	Total
warm	Hot water

References

[1] "IEA," 2020. [Online]. Available: https://www.iea.org/reports/world-energy-balances-overview.

[2] Bernardoni C, Binotti M, Giostri A. Techno-economic analysis of a closed OTEC cycles for power generation. Renewable Energy, 2019; 132: 1018-1033. https://doi.org/10.1016/j.renene.2018.08.007

[3] Avery WH, Wu C. Renewable Energy from the Ocean, A guide to OTEC. Oxford University Press, 1994. https://doi.org/10.1093/oso/9780195071993.001.0001

[4] Wang M, Jing R, Zhang H, Meng C, Li N, Zhao Y. An innovative Organic Rankine Cycle (ORC) based Ocean Thermal Energy Conversion (OTEC) system with performance simulation and multi-objective optimization. Applied Thermal Engineering, 2018; 145: 743-754. https://doi.org/10.1016/j.applthermaleng.2018.09.075

[5] Barberis S, Giugno A, Sorzana G, Lopes MFP, Traverso A. Techno-economic analysis of multipurpose OTEC power plants, in E3S Web of Conferences, 2019. https://doi.org/10.1051/e3sconf/201911303021

[6] Talluri L, Manfrida G, Ciappi L. Exergo-economic assessment of OTEC power generation, in Applied Energy Symposium. Pisa, Italy, 2020. https://doi.org/10.1051/e3sconf/202123801015

[7] Liu CC. Ocean thermal energy conversion and open ocean mariculture: The prospect of Mainland-Taiwan collaborative research and development. Sustainable Environment Research, 2018; 28: 267-273. https://doi.org/10.1016/j.serj.2018.06.002

[8] Kim AS, Kim H-J. Ocean Thermal Energy Conversione (OTEC) Past. Present and Progress, 2020. https://doi.org/10.5772/intechopen.86591

[9] Fiaschi D, Manfrida G, Rogai E, Talluri L. Exergoeconomic analysis and comparison between ORC and Kalina cycles to exploit low and medium-high temperature heat from two different geothermal sites. Energy Conversion and Management, 2017. https://doi.org/10.1016/j.enconman.2017.11.034

[10] Arsenyeva O, Klemeš JJ, Kapustenko P, Fedorenko O, Kusakov S, Kobylnik D. Plate heat exchanger design for the utilisation of waste heat from exhaust gases of drying process. Energy, 2021; 233: 121-186. https://doi.org/10.1016/j.energy.2021.121186

[11] Kærn MR, Modi A, Jensen JK, Haglind F. An Assessment of Transport Property Estimation Methods for Ammonia-Water Mixtures and Their Influence on Heat Exchanger Size. International Journal of Thermophysics, 2015. https://doi.org/10.1007/s10765-015-1857-8

[12] El-Sayed Y. Winter Annu. Meet. Am. Soc. Mech. Eng. 1988.

[13] Wilke CR. J. Chem. Phys. 1950.

[14] Razif NM, Mamat A, Lias I, Mohamed W. Thermophysical properties analysis for ammonia-water mixture of an organic Rankine cycle. Jurnal Teknologi, 2015.

[15] Dincer I. Rosen MA. EXERGY: Energy, Environment and Sustainable Development. Elsevier Science, 2005.

[16] Fiaschi D, Manfrida G, Petela K, Talluri L. Thermo-electric energy storage with solar heat integration: exergy and exergo-economic analysis. Energies, 2019. https://doi.org/10.3390/en12040648

[17] Turton R, Bailie R, Whiting W, Shaeiwitz J. Analysis, synthesis and design of chemical process. Prentice Hall PTR, 2003.

[18] "CEPCI, Chemical Engineering, Economic indicator," 11 07 2001/2015. [Online]. Available: https://www.chemengonline.com/2019-chemical-engineering-plant-cost-index-annual-average/v.